Identification and Functional Implications of Sodium/*Myo*-Inositol Cotransporter 1 in Pancreatic β-Cells and Type 2 Diabetes

Stephen Yu Ting Li, Sam Tsz Wai Cheng, Dan Zhang, and Po Sing Leung

Diabetes 2017;66:1258–1271 | DOI: 10.2337/db16-0880

***Myo*-inositol (MI), the precursor of the second messenger phosphoinositide (PI), mediates multiple cellular events. Rat islets exhibit active transport of MI, although the mechanism involved remains elusive. Here, we report, for the first time, the expression of sodium/*myo*-inositol cotransporter 1 (SMIT1) in rat islets and, specifically, β-cells. Genetic or pharmacological inhibition of SMIT1 impaired glucose-stimulated insulin secretion by INS-1E cells, probably via downregulation of PI signaling. In addition, SMIT1 expression in INS-1E cells and isolated islets was augmented by acute high-glucose exposure and reduced in chronic hyperglycemia conditions. In corroboration, chronic MI treatment improved the disease phenotypes of diabetic rats and islets. On the basis of our results, we postulate that the MI transporter SMIT1 is required to maintain a stable PI pool in β-cells in order that PI remains available despite its rapid turnover.**

Inositol is a naturally occurring cyclitol found in nine known isoforms, of which *myo*-inositol (MI) accounts for the largest population of active stereoisomers (1). Inositol is an important constituent of living cells that is known to take part in various cellular processes, including the development of peripheral nerves (2) and osteogenesis (3). Abnormal inositol metabolism has been reported in both type 1 and type 2 diabetes, as reflected by elevated urinary MI and D-*chiro*-inositol excretion (4–6). Indeed, MI supplementation has been documented to prevent the onset of gestational diabetes (7–9). Such findings have implicated MI in the regulation of glucose homeostasis. In addition to its role as an organic osmolyte in cells (10), MI is also a molecular precursor for the phosphoinositide (PI) second messenger system and perhaps a signaling molecule in its own right (11).

Rat pancreatic islets conduct active transport of MI (12), and exogenous MI has been reported to be necessary for the maintenance of β-cell function in rat islets (13). That is, in the absence of MI, rat islets were unresponsive to glucose stimulation, whereas increases in exogenous MI augmented insulin release after a glucose challenge (13). Pancreatic β-cell function and survival have also been shown to involve PI and its downstream effectors; specifically, glucose-stimulated activation of phospholipase C/protein kinase C (PLC/PKC) signaling has been previously reported to mediate second-phase insulin secretion by mobilizing Ca^{2+} ions stored in the endoplasmic reticulum (14). Meanwhile, activation of phosphoinositide 3-kinase (PI3K)–Akt signaling has been reported to promote β-cell function and survival (15,16). All of these findings suggest that MI may play a role in the intracellular signaling events of pancreatic β-cells.

Extracellular MI is taken up by membrane-bound inositol transporters (17). Two types of sodium-dependent MI cotransporters have been identified in humans, namely sodium/*myo*-inositol cotransporter 1 and 2 (*SMIT1* [*SLC5A3*] and *SMIT2* [*SLC5A11*], respectively; the latter is also known as sodium–glucose cotransporter [SGLT] 6). Both transporters are members of the solute carrier 5 gene family (18,19), and both transport MI along the concentration gradient of Na^+ in a stoichiometric ratio of 2 Na^+ ions for each MI molecule transported (20). SMIT1 shows higher specificity toward MI than SMIT2, which also transports D-glucose and D-*chiro*-inositol (21). Tissue expression studies

School of Biomedical Sciences, Faculty of Medicine, The Chinese University of Hong Kong, Hong Kong, China

Corresponding author: Po Sing Leung, psleung@cuhk.edu.hk.

Received 19 July 2016 and accepted 7 February 2017.

This article contains Supplementary Data online at http://diabetes.diabetesjournals.org/lookup/suppl/doi:10.2337/db16-0880/-/DC1.

S.T.W.C. and D.Z. contributed equally to this work.

have revealed widespread expression of both transporters in many human tissues, with particularly high expression levels in the brain and kidney cells (19,22).

Given that pancreatic islets are known to transport MI extensively (12) and the aforementioned recent findings showing that MI metabolism has been implicated in diabetic pathophysiology, the primary aim of the current study was to investigate the expression and function of inositol transporters in pancreatic islets and β-cells. In addition, we examined the mechanism by which MI may regulate β-cell function.

RESEARCH DESIGN AND METHODS

Animal Models

Male Zucker diabetic fatty (ZDF, *fa/fa*) rats, their age-matched littermates (Zucker lean [lean, *fa/*$^+$]), and Wistar rats (8–12 weeks old) were supplied by the Laboratory Animal Services Center of The Chinese University of Hong Kong. All rats were housed in a temperature- and humidity-controlled room under a 12-h light/dark cycle with ad libitum rodent chow (Teklad 7001, 4.4%; Harlan Teklad Global Diets) and water. All experimental procedures were approved by the Animal Experimentation Ethics Committee of The Chinese University of Hong Kong (Ref: # 14-025-MIS_5A).

MI Supplementation

ZDF rats (n = 5 per group) were assigned randomly to the treatment group (ZDF-MI), in which MI (Sigma-Aldrich, St. Louis, MO) supplementation was administered for 1 month in the drinking water (6 g · L^{-1}), or to the non–MI-treated control group (ZDF-Con). Water consumption was monitored daily to calculate mean intake of MI. A mean daily MI intake of 0.57 ± 0.04 mg/d · g (body wt) was recorded. Food and water intake and body weight were measured weekly.

In Vivo Glucose Homeostasis

A glucometer (Bayer Corporation, Robinson Township, PA) was used to measure blood glucose in blood samples drawn from the tail vein. Intraperitoneal glucose tolerance tests (IPGTTs) were administered wherein, after a 6-h fast, rats were challenged with glucose (2 g · kg^{-1}), and blood glucose was measured 0, 15, 30, 60, 90, and 120 min thereafter. For insulin tolerance tests (ITTs), after a 4-h fast, rats were challenged with insulin (1.25 units/kg body wt) by intraperitoneal administration, and blood glucose was measured 0, 15, 30, and 60 min thereafter. Area under the curve (AUC) values for blood glucose were then calculated.

Immunohistochemistry, Pancreatic Islet Isolation, β-Cell Purification, and Treatments

Pancreata were embedded in O.C.T. compound (Sakura, Tokyo, Japan) and were frozen. Cryostat sections (6 μm thick) were cut, mounted, and blocked in 2% BSA (Sigma-Aldrich) with 0.1% Triton X-100 (Sigma-Aldrich) for 30 min at room temperature. For the α- and β-cell analyses, sections were probed with rabbit polyclonal anti-insulin antibody (1:250; Santa Cruz Biotechnology, Santa Cruz, CA) and mouse monoclonal anti-glucagon antibody (1:250; Abcam, Cambridge, MA) and incubated for 2 h at room temperature with Alexa Fluor 568 donkey anti-rabbit antibody (1:250; Life Technologies, Carlsbad, CA) and Alexa Fluor 488 goat anti-mouse antibody (1:250; Life Technologies). For the β-cell proliferation analyses, sections were probed at 4°C with guinea pig polyclonal anti-insulin antibody (1:250; Life Technologies) and rabbit polyclonal anti-Ki67 antibody (1:250; Abcam) and then incubated for 2 h at room temperature with Alexa Fluor 488 goat anti-guinea pig antibody (1:250) and Alexa Fluor 568 donkey anti-rabbit antibody (1:250). Immunolabeling was analyzed by assessing the ratios of areas occupied by the red and green fluorescent signals within each islet by using ImageJ software (National Institutes of Health, Bethesda, MD).

Intact islets were isolated by injecting collagenase P (Roche, Mannheim, Germany) intraductally into harvested pancreata as described previously (23). Isolated islets were cultured overnight before treatment with 5.6 or 28 mmol/L D-glucose (Sigma-Aldrich) in the presence of 0.5 mmol/L phlorizin (Sigma-Aldrich) and/or 500 μg/mL MI for the designated periods of time. For purification of pancreatic β-cells, isolated islets were dispersed, and β-cells were isolated by flow cytometry as previously described (24). β-Cell purity was further assessed by flow cytometry using intracellular staining with Alexa Fluor 647 Mouse Anti-Insulin (BD Biosciences, San Diego, CA) and PE Mouse Anti-Glucagon (BD Biosciences) as previously described (25).

INS-1E Cell Culture and Treatment

The insulinoma cell line INS-1E cell, a gift from Dr. Pierre Maechler (26), was cultured in a humidified chamber with 5% CO_2 in RPMI 1640 medium (11.2 mmol/L glucose) supplemented with 10% FBS, 1 mmol/L sodium pyruvate, 50 μmol/L 2-mercaptoethanol, 10 mmol/L HEPES, 100 units/mL penicillin, and 100 μg/mL streptomycin (all from Invitrogen, Waltham, MA). Cultures were passaged once weekly by gentle trypsinization. INS-1E cells were treated with 11.2 mmol/L or 28 mmol/L glucose, 0.5 mmol/L phlorizin, and/or 500 μg/mL MI for the experimentally indicated periods of time.

Knockdown of *SMIT1* Transcription

SMIT1 expression was suppressed with small interfering RNAs (siRNAs) for rat SMIT1 (constructed by Life Technologies, Hong Kong). INS-1E cells were transfected with siRNA-SMIT1 oligos or siRNA negative control oligos with Lipofectamine RNAi Max transfection reagent (Invitrogen) for 48 h, according to the manufacturer's instructions. The sequences of the knockdown and control oligos are listed in Supplementary Table 1. Knockdown efficiency was determined by measuring SMIT1 expression levels in real-time PCRs and immunoblotting (Supplementary Fig. 2).

Glucose-Stimulated Insulin Secretion and Insulin Content Measurement

Glucose-stimulated insulin secretion (GSIS) was performed, as described previously (23), to assess β-cell function. Treated cells or isolated islets were normalized for their

basal insulin-secreting status by preincubation in Krebs-Ringer bicarbonate buffer (KRBB) that contains 1.6 mmol/L D-glucose for 1 h. After normalization, the cells and islets were incubated in KRBB with 1.6 mmol/L D-glucose for 1 h, and the buffer was collected. The cells and islets were incubated in fresh KRBB with 16.7 mmol/L D-glucose for 1 h, during which stimulated insulin secretion was measured. For the measurement of intracellular insulin content, treated cells or isolated islets incubated in HCl-ethanol overnight at −20°C were homogenized and further incubated overnight at −20°C. Homogenized samples were centrifuged, and the supernatant was neutralized with 1 mol/L Tris (pH 7.5). ELISAs with a specific rat insulin ELISA kit (Antibody and Immunoassay Services at The University of Hong Kong) were used to quantify the amount of insulin released or intracellular insulin content in the collected buffer samples.

Cytosolic Calcium Measurement

INS-1E cells were incubated for 30 min in a cell incubator in KRBB with 16.7 mmol/L D-glucose and 5 μmol/L Fluo-8 AM (Abcam). After incubation, cells were rinsed twice with PBS and treated with 28 mmol/L D-glucose. Fluorescence signals were monitored continuously for 7 min after glucose administration at 490 and 525 nm excitation and emission wavelength, respectively. Results were expressed as the F-to-F_0 ratio, with F_0 being the basal fluorescence intensity in the unstimulated condition.

Quantification of Intracellular MI Level

The intracellular MI level was quantified by high-performance liquid chromatography tandem mass spectrometry (HPLC/MS), as previously described (27). In brief, treated cells were extracted with 3 volumes of acetonitrile to precipitate proteins. The precipitated proteins were removed by centrifugation, and the samples were diluted in HPLC water before HPLC/MS analysis. Separation of samples was performed in HPLC, with the protocol of an isocratic gradient of 95% HPLC water to 5% acetonitrile. Quantification was done by analyzing the multiple reaction monitoring transitions of 178.8 → 86.4 from the coupled triple quadrupole tandem MS analysis, operating in negative-ion mode. Intracellular MI levels were normalized to total protein levels.

RT-PCR and Real-time PCR analysis

TRIzol reagent (Invitrogen) was used for total RNA extraction from pancreatic islets and cells, according to the manufacturer's instructions. First-strand cDNA was reverse transcribed with a PrimeScript reverse transcriptase master mix kit (Takara Bio Inc., Shiga, Japan). Gene expression was analyzed by PCR analysis or real-time PCR quantification, wherein cDNA samples were combined with SYBR Green QPCR master mix (Applied Biosystems, Carlsbad, CA) and specific primers (Supplementary Table 1). Relative gene expression was analyzed by the comparative threshold cycle method ($2^{-\Delta\Delta CT}$) and normalized to β-actin.

Western Blotting

Islet and cell proteins were extracted with the CytoBuster Protein Extraction Reagent (Novagen, Darmstadt, Germany). Extracted proteins were fractionated by 10% SDS-PAGE and transferred to nitrocellulose membranes (Bio-Rad, Munich, Germany), which were blocked with 5% milk and then probed with anti-SMIT1 (Novus, St. Louis, MO), anti-AKT (Cell Signaling Technology, Beverly, MA), anti–phospho-AKT (Ser473; Cell Signaling Technology), anti-ERK1/2 (Cell Signaling Technology), anti–phospho-ERK1/2 (Thr202/Tyr204; Cell Signaling Technology), or anti–β-actin (Santa Cruz Biotechnology) antibodies. Horseradish peroxide–conjugated secondary antibodies were applied to the membranes after washing. Labeled protein bands were visualized on autoradiography films (Fujifilm, Tokyo, Japan) after application of enhanced chemiluminescence detection reagent (GE Healthcare, Piscataway, NJ). The protein bands were analyzed with ImageJ software. Protein bands were normalized to β-actin protein levels.

Lipid Extraction and Quantification of Phosphatidylinositol 4,5-Bisphosphate and Inositol Triphosphate Levels

Lipids were extracted from treated cells as previously described (28). Briefly, cells were scraped with cold 0.5 mol/L trichloroacetic acid and centrifuged. The cellular pellets were washed with 5% trichloroacetic acid/1 mmol/L EDTA. Neutral lipids were removed from the cell pellets by addition of methanol:chloroform (2:1), and acidic lipids were extracted with methanol:chloroform:12 mol/L HCl (80:40:1). The lower organic phases were collected after phase separation with chloroform/0.1 mol/L HCl and then vacuum dried in a vacuum dryer for subsequent assays.

Intracellular phosphatidylinositol 4,5-bisphosphate (PIP_2) levels were quantified with a PIP_2 Mass ELISA Kit (Echelon Bioscience Inc., Salt Lake City, UT), according to the manufacturer's instructions. Briefly, extracted lipids were dissolved in PBS with 0.25% protein stabilizer (kit supplied). The resuspension was probed with a PIP_2 detector protein (kit supplied) for 1 h and then incubated in a 96-well PIP_2-coated microplate. A peroxidase-linked secondary detection reagent was applied to detect plate-bound PIP_2-detector protein, generating colorimetric signals measured at 450 nm. PIP_2 levels were expressed as pmol/10,000 cells or pmol/number of islets, according to calculations based on the standard curve generated. Intracellular inositol triphosphate (IP_3) levels analyses were performed with a Rat IP_3 ELISA Kit (CUSABIO Biotech, Wuhan, China), according to the manufacturer's instructions.

Data Analysis

Group data are reported as means ± SEMs. Differences between groups were detected by Student unpaired two-tailed *t* tests or one-way ANOVAs, followed by Tukey post hoc tests, wherein $P < 0.05$ was considered statistically significant.

RESULTS

MI Transporters Were Expressed in Islets and β-Cells

Expression of both *SMIT1* and *SMIT2* was detected in freshly isolated rat pancreatic islets and INS-1E cells by

RT-PCR assays (Fig. 1*A* and *B*). Quantitative PCR analysis revealed that expression of *SMIT1* in INS-1E cells was 300-fold higher than that of *SMIT2* (Fig. 1*C*), with a primer extension efficiency of 96.3% for *SMIT1* and 98.1% *SMIT2*. Immunoblot analysis further demonstrated an 80-kDa SMIT1-specific antibody-reactive protein band in assays of samples from rat pancreatic islets and INS-1E cells (Fig. 1*D*). Further analyses of the purified rat pancreatic β-cells revealed a twofold higher *SMIT1* mRNA expression in the β-cell population than in that of the non–β-cell population (Fig. 1*E*). A purity of 97.3% was achieved (Fig. 1*F*), indicating that *SMIT1* is specifically expressed at a high level in rat pancreatic β-cells.

Acute High-Glucose Exposure and Early Hyperglycemic State Induce SMIT1 Expression

MI is known to play an important role in regulating intracellular osmolarity and fluid balance (19). To assess the osmoregulatory role of SMIT1, INS-1E cells were treated with 28 mmol/L mannitol for 6 h. *SMIT1* mRNA expression was significantly increased (Fig. 2*A*). Further immunoblot analysis revealed that the protein expression was also upregulated in INS-1E cells treated with 28 mmol/L mannitol for 12 h (Fig. 2*B*) relative to the controls. Similarly, exposure of INS-1E cells to acute high-glucose concentrations (28 mmol/L glucose for 6 h) increased *SMIT1* mRNA expression by twofold relative to controls (Fig. 2*C*). In addition, the protein expression level of SMIT1 was also augmented in INS-1E cells treated with 28 mmol/L glucose for 12 h (Fig. 2*D*). To exclude the effect of insulin on SMIT1 expression under high-glucose conditions, INS-1E cells were further treated with 5 μmol/L GSK1838705A, an insulin receptor blocker. The results revealed that the insulin receptor blocker failed to reduce the augmented SMIT1 expression in high-glucose–treated INS-1E cells

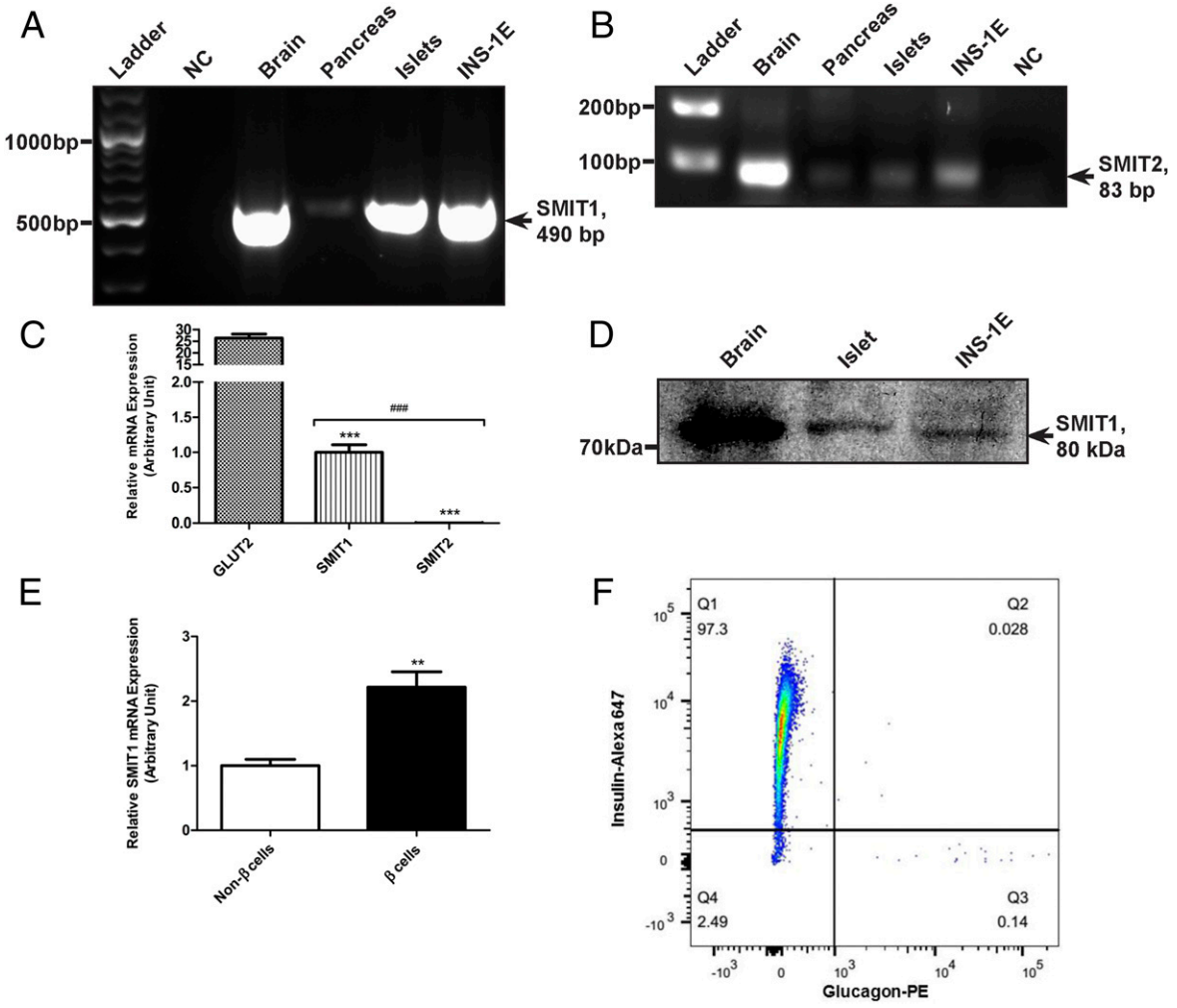

Figure 1—Expression of inositol transporters in rat islets, INS-1E, pancreas, and brain tissues. RT-PCR analysis for the mRNA expression of *SMIT1* (*A*) and *SMIT2* (*B*). NC, negative control. *C*: Quantitative real-time PCR analysis for the mRNA expression of *SMIT1* and *SMIT2* in INS-1E cells. *D*: Western blot analysis for the protein expression of SMIT1 in islets and INS-1E; brain was used as a positive control for SMIT1 expression with a molecular weight of ~80 kDa. *E*: Quantitative real-time PCR analysis for the relative expression of *SMIT1* mRNA expression in purified β-cell population and non–β-cell population in islets. *F*: Flow cytometry analysis for the purity of isolated β-cells. PE, R-phycoerythrin. ***P < 0.001 vs. *GLUT2*; ###P < 0.001 vs. *SMIT1*; **P < 0.01 vs. non–β-cells.

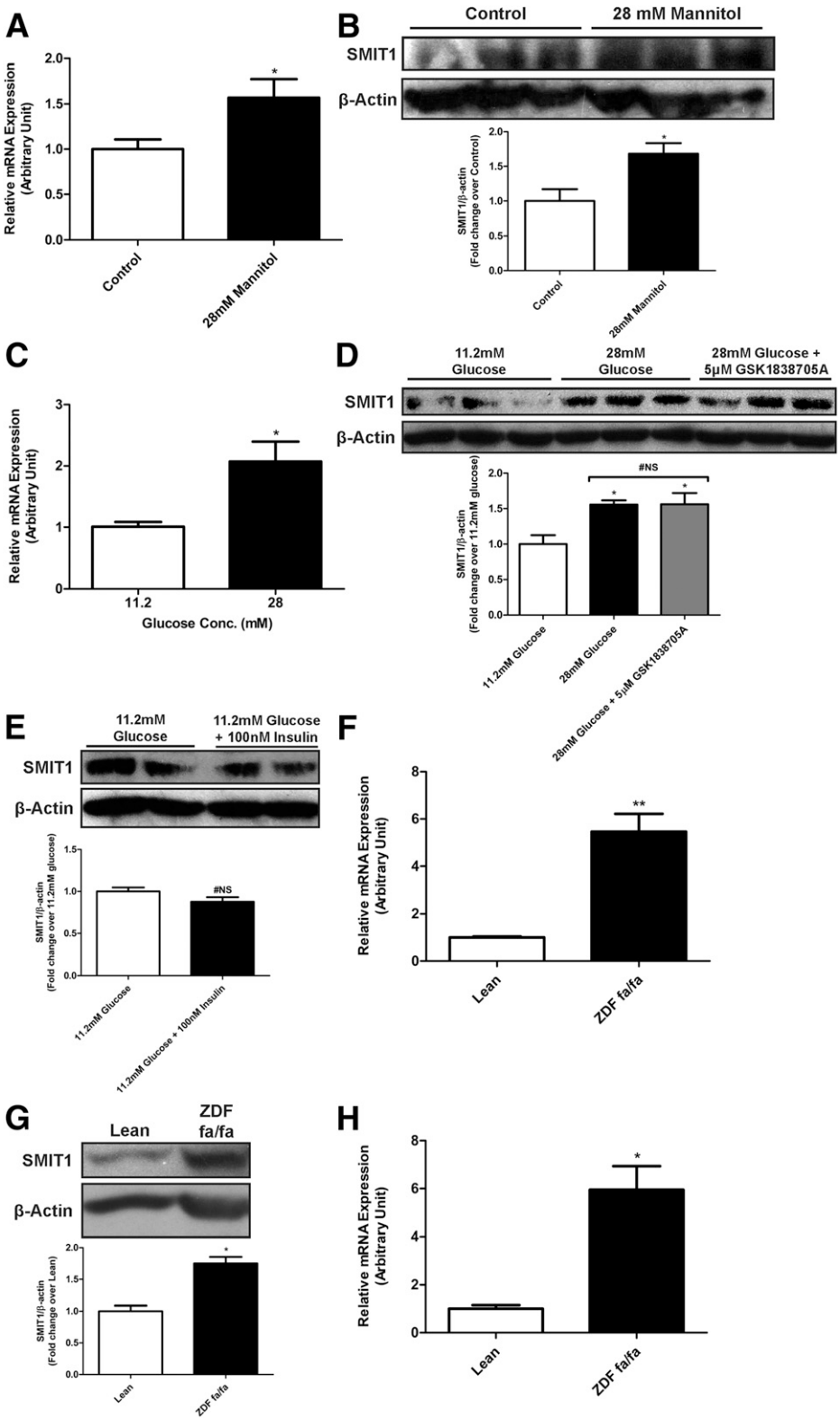

Figure 2—*A*: Real-time PCR analysis of *SMIT1* mRNA expression in INS-1E cells treated with 28 mmol/L mannitol for 6 h. *B*: Western blot of SMIT1 protein expression in INS-1E cells exposed to 28 mmol/L mannitol for 12 h. *C*: Real-time PCR analysis of *SMIT1* mRNA expression in INS-1E cells treated with 11.2 mmol/L or 28 mmol/L D-glucose for 6 h. *D*: Western blot analysis of SMIT1 protein expression in INS-1E cells treated with 11.2 mmol/L glucose, 28 mmol/L glucose, or 28 mmol/L glucose plus 5 μmol/L GSK1838705A for 12 h. *E*: Western blot analysis of SMIT1 protein expression in INS-1E cells treated with 100 nmol/L insulin. *SMIT1* mRNA expression (*F*) and protein expression (*G*) in islets isolated from 11- to 12-week-old and 7- to 8 week-old (*H*) ZDF rats, in relation with their age-matched littermates (n = 4/group). Means ± SEM from at least three independent experiments are shown. #NS, nonsignificant. $^*P < 0.05$, $^{**}P < 0.01$ vs. respective controls.

(Fig. 2*D*). Furthermore, treatment of insulin alone on INS-1E cells did not have a significant effect on SMIT1 expression (Fig. 2*E*).

We further examined the effect of hyperglycemia on SMIT1 expression using the ZDF diabetic rat model. Our results showed that islets from 11- to 12-week-old ZDF diabetic rats expressed *SMIT1* mRNA fivefold higher than that observed in islets from lean rats (Fig. 2*F*), consistent with a response to extracellular hypertonic stress. Immunoblot analysis of islets from 11- to 12-week-old ZDF diabetic rats also revealed an increased SMIT1 expression (Fig. 2*G*). Surprisingly, we found that *SMIT1* mRNA expression level in islets from 7- to 8-week-old ZDF diabetic rats was also upregulated (Fig. 2*H*).

Chronic High-Glucose Exposure and Chronic Hyperglycemic Conditions Suppress SMIT1 Expression

Given that diabetes is associated with abnormal inositol metabolism (4–6), we hypothesized that chronic exposure to high-glucose and/or chronic hyperglycemia would reduce SMIT1 expression. Our quantitative PCR experiment demonstrated significant decreases in *SMIT1* mRNA expression of INS-1E cells after a 48-h or 72-h high-glucose treatment (Fig. 3*A*). Levels of SMIT1 protein were also downregulated in INS-1E cells in the 72-h high-glucose–treatment group (Fig. 3*B*). In contrast to the augmented *SMIT1* mRNA expression in early-stage diabetic rat islets, we found that the pancreatic islets of more mature ZDF rats (24–36 weeks old) displayed significantly reduced *SMIT1* mRNA expression (Fig. 3*C*). Immunoblot analysis also revealed a reduction in SMIT1 protein expression in mature ZDF rat islets (Fig. 3*D*). To rule out the influence of age on the downregulation of SMIT1 expression, we compared the expression of *SMIT1* mRNA in islets from young lean rats (8 weeks old) and more mature lean rats (24–36 weeks old). The results showed that the respective *SMIT1* mRNA expression levels were comparable (Fig. 3*E*), indicative of age independence.

Pharmacological and Genetic Inhibition of SMIT1 Impair GSIS and Reduce Insulin Content

We next examined whether SMIT1 is involved in the regulation of insulin secretory function. To address this issue, we used phlorizin, a nonspecific inhibitor of SGLT (29), to study SMIT1-mediated GSIS. As a first step, an expression profile of SGLT family in INS-1E was performed to determine the presence of any other SGLT family members, the activities of which could be inhibited by phlorizin. RT-PCR experiments confirmed that INS-1E cells express *SMIT1* mRNA and, to a lesser extent, *SMIT2* mRNA, but the other transporter family member mRNAs were not detected (Supplementary Fig. 1). SMIT inhibition with phlorizin (0.5 mmol/L) for 48 h impaired GSIS in INS-1E cells cultured in a normal glucose (11.2 mmol/L) condition, and no further impairment of GSIS was observed in cells cultured in high-glucose (28 mmol/L) conditions (Fig. 4*A*). Subsequent incubation of the treated cells in a phlorizin-free solution with 500 μg/mL MI for 3 h rescued normal GSIS in phlorizin-treated cells (Fig. 4*B*). MI supplementation produced fold-magnitude changes in the GSIS of the treated cells (see histogram in Fig. 4*C*). Rat pancreatic islets that were treated with 0.5 mmol/L phlorizin for 48 h also showed impaired GSIS (Fig. 4*D* and *E*). Moreover, phlorizin-treated cells exhibited a significant reduction in intracellular insulin content (Fig. 4*F*). When the insulin secretion level was expressed as the percentage of insulin content, its level was still significantly reduced, indicating that insulin biosynthesis and secretion were both affected (Fig. 4*G*).

To further confirm the functional role of SMIT1 on GSIS, we also performed siRNA-mediated knockdown of SMIT1 in INS-1E cells. Our results showed that transfection of INS-1E cells with SMIT1-specific siRNA led to reductions in 75% of *SMIT1* mRNA expression and 50% of SMIT1 protein expression as well as 50% of the intracellular MI level (Supplementary Fig. 2). This SMIT1 knockdown consistently resulted in impaired GSIS relative to control siRNAs (Fig. 4*H* and *I*). Furthermore, SMIT1 knockdown also significantly decreased intracellular insulin content (Fig. 4*J*) and secretion level expressed as a percentage of insulin content (Fig. 4*K*).

SMIT1 Knockdown Reduces PIP_2 Levels and Downregulates PI Signaling

Given that MI is a major precursor for PI (11), we hypothesized that alterations in SMIT1 activity would modulate intracellular PI levels. Firstly, RT-PCR experiments were performed to demonstrate that INS-1E cells are able to express the major enzymes involved in the conversion of MI to PI (Supplementary Fig. 3). Secondly, our ELISA results confirmed that SMIT1 knockdown with siRNA-SMIT1 reduced intracellular PIP_2 levels in INS-1E cells (Fig. 5*A*). We next sought to investigate whether the downstream of PI signaling cascades would also be affected by the deficiency of SMIT1. INS-1E cells with SMIT1 knockdown displayed a significant reduction in the intracellular IP_3 level, but the transfected cells were unresponsive toward a high-glucose challenge at 28 mmol/L for 5 min (Fig. 5*B*). Furthermore, SMIT1-knockdown INS-1E cells failed to exhibit an increase in intracellular $[Ca^{2+}]$ in response to 28 mmol/L glucose treatment (Supplementary Fig. 4). Given that SMIT1 knockdown impaired PIP_2 signaling cascades, we next studied its effect on PI3K/phosphatidylinositol 3,4,5-triphosphate (PIP_3)/Akt signaling cascades. AKT phosphorylation was used as the first reporter. SMIT1 knockdown reduced basal AKT phosphorylation and stimulated the phosphorylation level upon acute insulin treatment (100 nmol/L) in INS-1E cells (Fig. 5*C*). Similarly, ERK phosphorylation was reduced at basal and insulin-stimulated conditions (Fig. 5*D*). Meanwhile the expression of immediate downstream target genes of the PI3K/Akt signaling pathway was further used as a readout for any potential disturbances over the signaling cascades. Our results demonstrated that

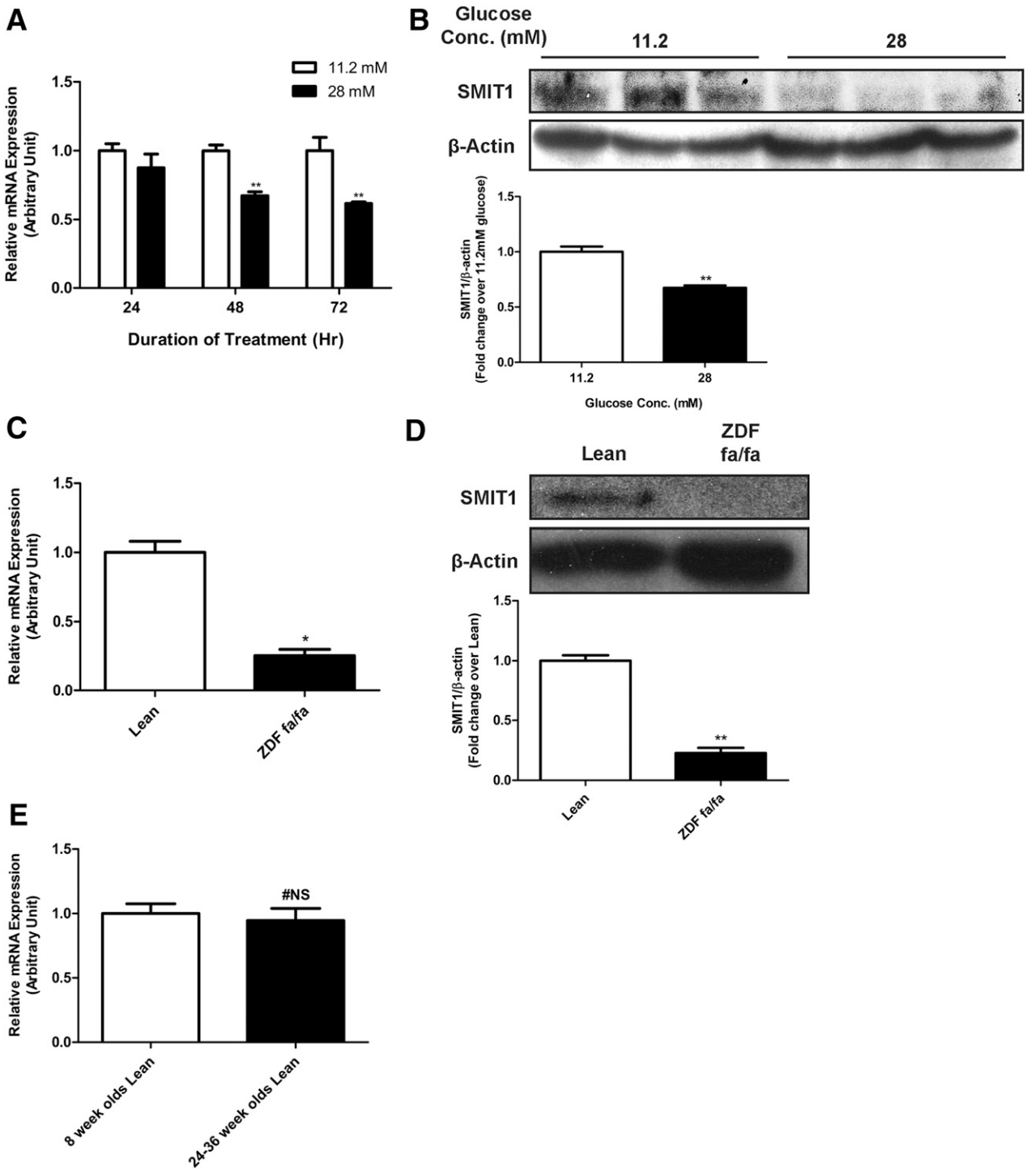

Figure 3—*A*: Real-time PCR of *SMIT1* mRNA expression in INS-1E cells cultured 24, 48, and 72 h after high-glucose (28 mmol/L) exposure. *B*: Western blot analysis of SMIT1 protein expression in INS-1E cells under 72-h high-glucose treatment. *C*: Real-time PCR of *SMIT1* mRNA expression in islets isolated from 24- to 36-week-old ZDF rats and their age-matched littermates (n = 4/group). *D*: SMIT1 protein expression in islets isolated from 24- to 36-week-old ZDF rats and their age-matched littermates (n = 4/group). *E*: *SMIT1* mRNA expression in islets isolated from 8-week-old and 24- to 36-week-old ZDF rats. Means ± SEM of at least three independent experiments are shown. #NS, nonsignificant. *$P < 0.05$, **$P < 0.01$ vs. respective controls.

SMIT1 knockdown also reduced those transcription of genes that encode proteins responsible for β-cell function and known downstream transcription targets of PI3K/Akt signaling (30,31), namely *Pdx1*, *GLUT2*, and *Ins2* (Fig. 5*E*–*G*). Interestingly, SMIT1 knockdown differentially altered insulin/IGF-I signaling in INS-1E cells. Specifically, we found that the mRNA expression levels of *Irs1* and *Irs2* were decreased and increased, respectively (Fig. 5*H* and *I*).

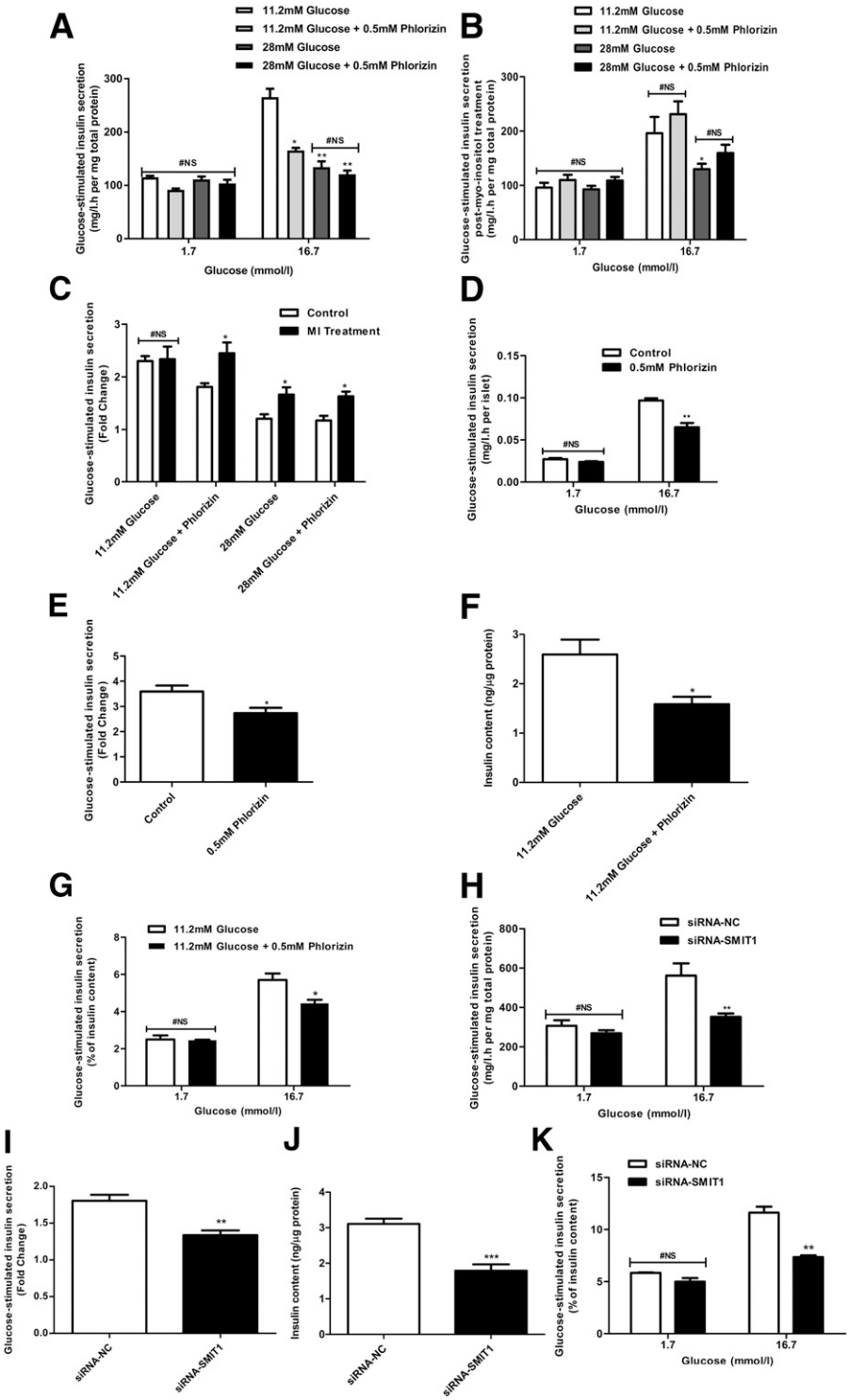

Figure 4—GSIS analysis for INS-1E cells treated with 11.2 mmol/L normal glucose, 11.2 mmol/L glucose with 0.5 mmol/L phlorizin, 28 mmol/L high glucose, or high glucose with 0.5 mmol/L phlorizin for 48 h. GSIS was conducted under low-glucose (1.7 mmol/L) and high-glucose (16.7 mmol/L) conditions. *A*: ELISA-determined insulin concentrations in cell buffer samples are shown. *B*: GSIS analysis for INS-1E cells treated as in *A* and then treated with 500 μg/mL MI for 3 h. *C*: Histogram shows the effects of MI treatment relative to the non–MI-treated control group. *D* and *E*: GSIS analysis for islets isolated from Wister rats treated with 0.5 mmol/L phlorizin in the presence of 5.6 mmol/L glucose under low-glucose (1.7 mmol/L) and high-glucose (16.7 mmol/L) stimulation conditions. *F*: Intracellular insulin content analysis is shown for INS-1E cells treated with 0.5 mmol/L phlorizin. *G*: Insulin secretion level of phlorizin-treated cells expressed as percentage of insulin content. *H* and *I*: GSIS analysis for INS-1E cells transfected with siRNA-SMIT1 or negative control (NC) siRNAs. *J*: Intracellular insulin content analysis for INS-1E cells transfected with siRNA-SMIT1 or negative control siRNAs. *K*: Insulin secretion level of siRNA-SMIT1–transfected cells expressed as percentage of insulin content. Means ± SEM of at least three independent experiments are shown. #NS, nonsignificant. **P* < 0.05, ***P* < 0.01, ****P* < 0.001 vs. respective controls.

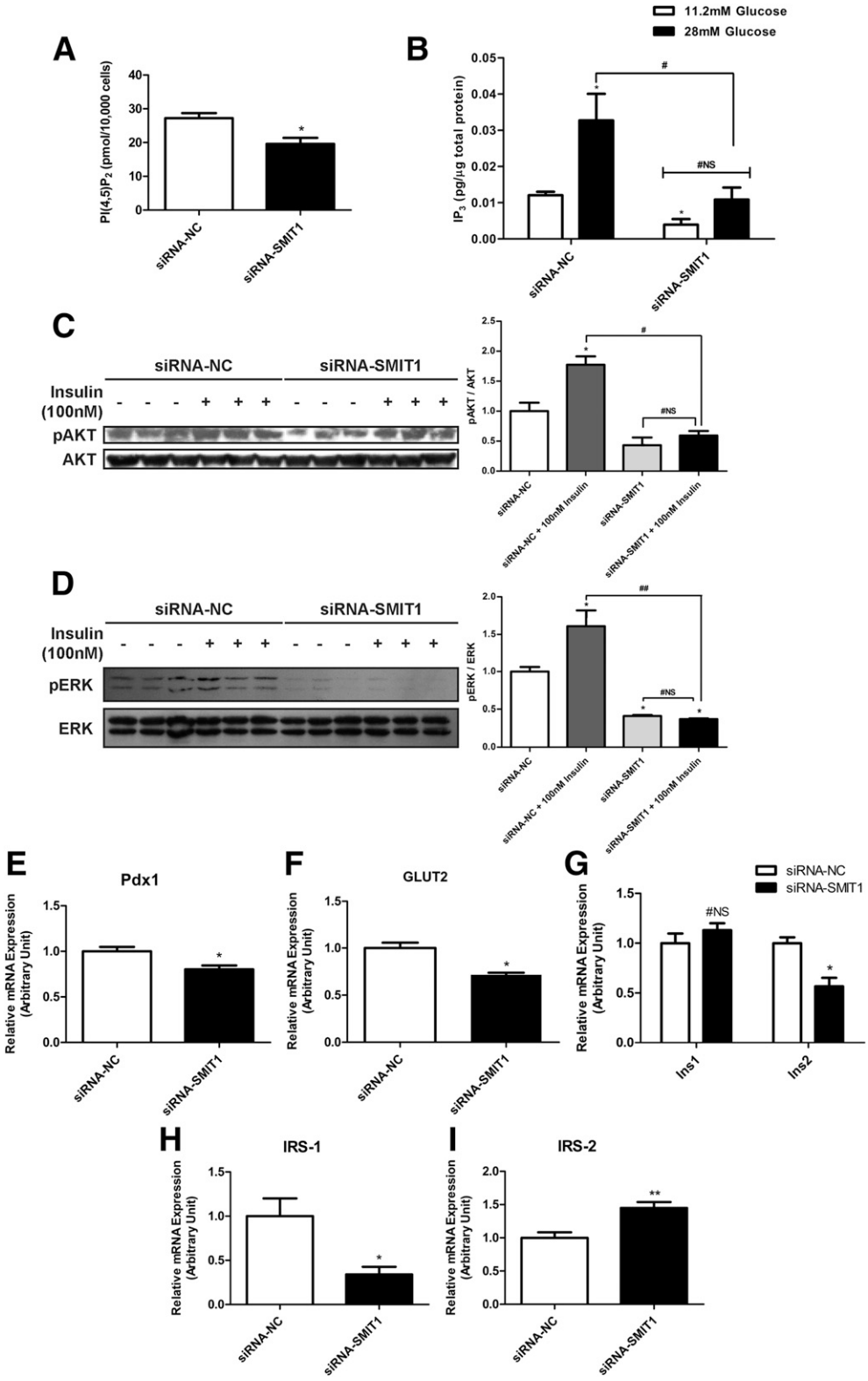

Figure 5—*A*: ELISA analysis of intracellular PIP_2 levels in INS-1E cells transfected with siRNA-SMIT1 (SMIT knockdown) or negative control (NC) siRNAs. *B*: ELISA analysis of intracellular IP_3 levels in INS-1E cells transfected with siRNA-SMIT1 or negative control siRNAs in response to 28 mmol/L glucose concentrations. *C*: Phosphorylated AKT (pAKT) and total AKT expression were analyzed and quantified by Western blotting; the pAKT-to-total AKT ratios were calculated and were relatively compared. *D*: Phosphorylated ERK (pERK) and total ERK expression were analyzed and quantified by Western blotting; the pERK-to-total ERK ratios were calculated and were relatively compared. Real-time PCR analysis is shown for the mRNA expression of genes encoding β-cell functional proteins, namely *Pdx1* (*E*), *GLUT2* (*F*), *Ins1* and *Ins2* (*G*), *IRS-1* (*H*), and *IRS-2* (*I*). Means ± SEM of at least three independent experiments are shown. #NS, nonsignificant. $^{*}P < 0.05$, $^{**}P < 0.01$ vs. respective controls; $\#P < 0.05$, $\#\#P < 0.01$ vs. treated siRNA-NC controls.

MI Supplementation Improves Glucose Homeostasis in ZDF Rats

For the in vivo functionality assessments, we sought to examine whether MI supplementation is beneficial to diabetic conditions. Our results showed that treatment of pancreatic islets isolated from 24- to 36-week-old ZDF rats with 500 μg/mL MI for 48 h resulted in a rescue of GSIS (Fig. 6*A* and *B*). For in vivo MI supplementation (0.57 ± 0.04 mg/d · g for 1 month), the treatment did not alter body weight or food or water intake between MI-treated and untreated ZDF rats (Supplementary Table 2). However, the supplementation improved glucose tolerance in 24- to 36-week-old ZDF rats, as reflected by reduced fasting blood glucose level (Fig. 6*C*) and improved IPGTTs with reduced glucose concentrations (AUC results) relative to untreated age-matched ZDF controls (Fig. 6*D* and *E*). However, we did not observe any significant differences in insulin sensitivity between MI-treated and untreated ZDF rats, as evidenced by ITTs (Fig. 6*F* and *G*) and HOMA-insulin resistance data (Fig. 6*H*).

MI Supplementation Preserves Islet Morphology, Improves Islet Function, and Enhances PI Signaling in ZDF Rats

We also proceeded to examine the direct pancreatic islet function of MI-treated rats and found that islets isolated

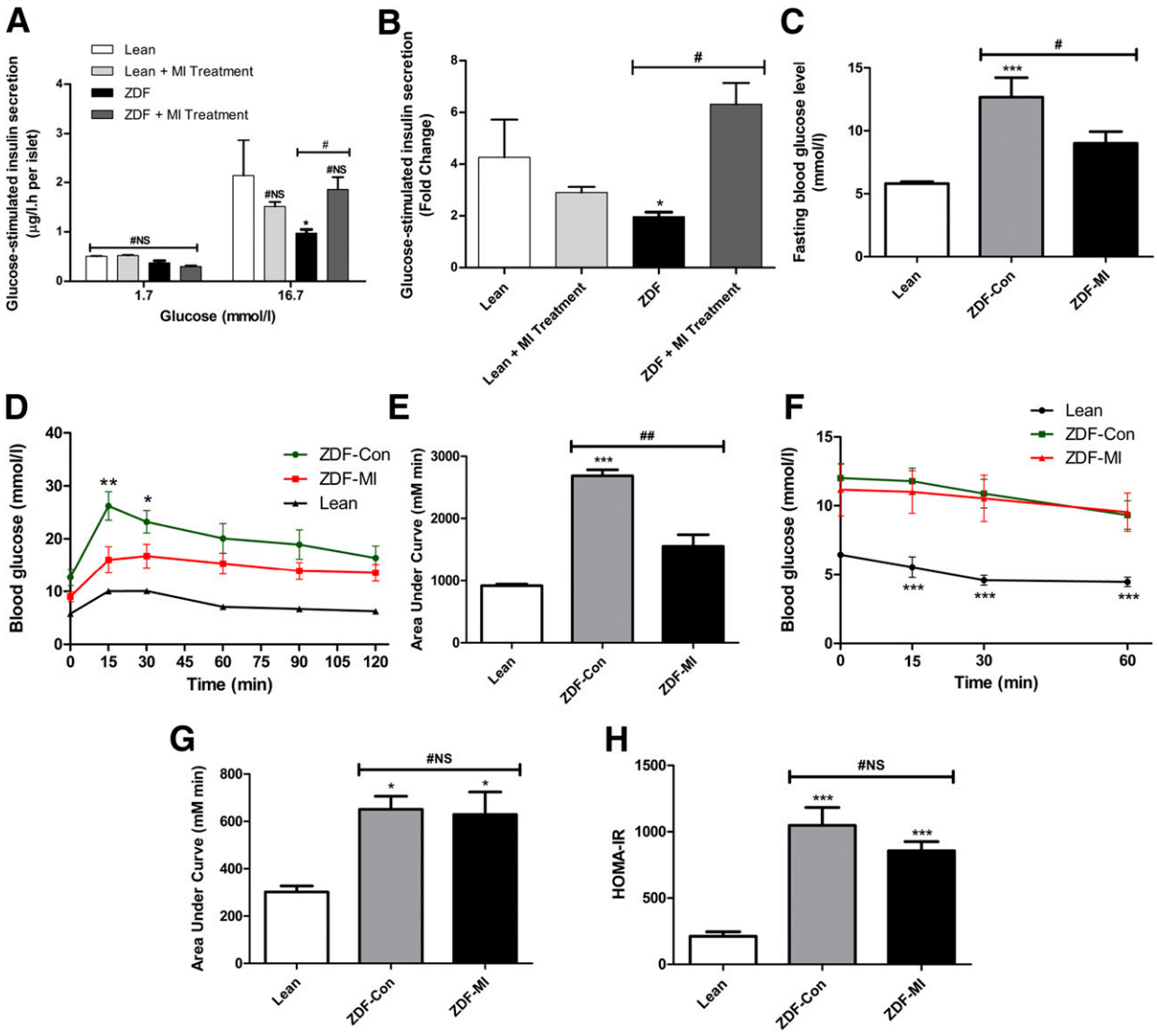

Figure 6—GSIS results for islets isolated from 24- to 36-week-old ZDF rats and lean rats treated with 500 μg/mL MI for 48 h. *A* and *B*: GSIS was conducted under low-glucose (1.7 mmol/L) and high-glucose (16.7 mmol/L) conditions, and insulin concentrations in buffer samples were quantified by ELISAs. Fasting blood glucose level (*C*) and IPGTT results for rats that received 1 month of MI supplementation treatment (0.57 ± 0.04 mg/d · g); blood glucose concentrations during the IPGTT (*D*) and the AUC (*E*) are shown. Blood glucose concentrations during ITTs (*F*) and AUC for glucose concentrations (*G*) are shown. *H*: HOMA-insulin resistance index for each experimental group was calculated. Means ± SEM of at least three independent experiments are shown (n = 3–6/group). #NS, nonsignificant. *$P < 0.05$, **$P < 0.01$, ***$P < 0.001$ vs. lean controls; #$P < 0.05$, ##$P < 0.01$ vs. non–MI-treated controls.

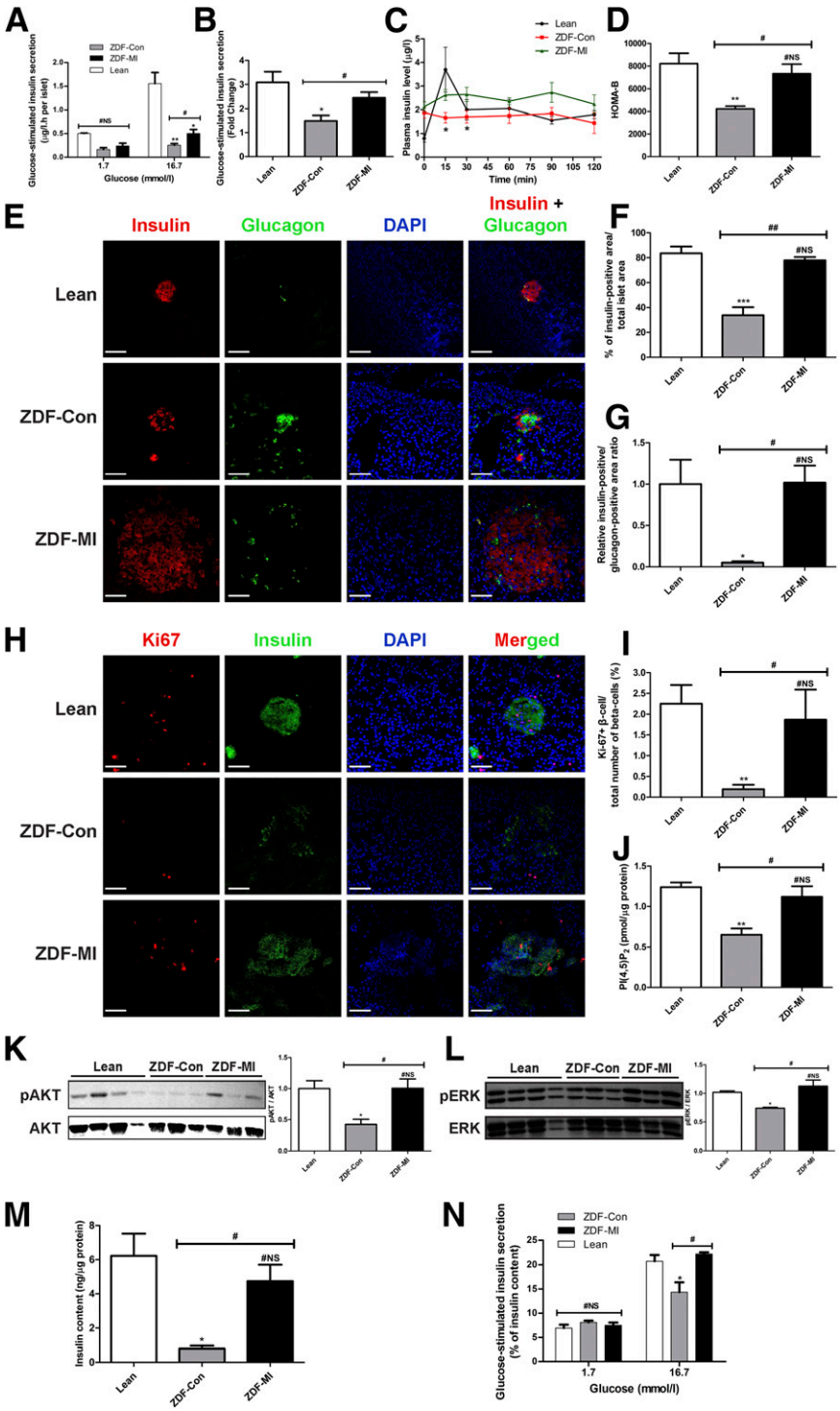

Figure 7—*A* and *B*: GSIS results for islets isolated from rats treated with MI supplementation for 1 month. *C*: Serum insulin concentrations during IPGTT are shown. *D*: HOMA-B index was calculated for each group. *E*: Immunofluorescent assessment with insulin (red), glucagon (green), and DAPI (blue) in pancreatic sections from rats treated as described above. *F*: Bar chart shows the percentage of β-cell area/total islet area. *G*: Bar chart shows the mean area of α-cell–to–β-cell ratio per pancreatic cross-section. *H*: Immunofluorescent assessment with Ki-67 (red), insulin (green), and DAPI (blue) in pancreatic sections from rats treated as described above. *I*: Bar chart shows the percentage of Ki-67 positive β-cell/total number of β-cells. *J*: ELISA analysis of intracellular PIP_2 levels in islets from rats treated as described above. *K*: Expression of phosphorylated AKT (pAKT) and total AKT were quantified by Western blotting; the pAKT-to-total AKT ratios were calculated and relatively compared. *L*: Expression of phosphorylated ERK (pERK) and total ERK were quantified by Western blotting; the pERK-to-total ERK ratios were calculated and relatively compared. *M*: Intracellular insulin content analysis for islets from rats treated as described above. *N*: Insulin secretion level, expressed as the percentage of insulin content of islets from rats treated as described above. Means ± SEM of at least three independent experiments are shown (n = 3–6/group). Scale bars = 100 μm. #NS, nonsignificant. *$P < 0.05$, **$P < 0.01$, ***$P < 0.001$ vs. lean controls; #$P < 0.05$, ##$P < 0.01$ vs. non-MI treated controls.

from the MI treatment group exhibited improved GSIS compared with that of untreated ZDF control islets (Fig. 7*A* and *B*). Consistently, there was a significant increase in serum insulin concentration in the MI-treated ZDF rats at 15 and 30 min after glucose administration compared with that of the untreated ZDF rats (Fig. 7*C*), indicating an improvement in islet function, as further reflected by an increased HOMA-B index (Fig. 7*D*). To investigate the beneficial effects of MI supplementation on islet function, islet morphology was studied by characterizing the β-cell–to–α-cell ratio and β-cell proliferation using immunohistochemical staining. MI supplementation remarkably increased the β-cell–to–α- cell ratio (Fig. 7*E*–*G*) and β-cell proliferation in ZDF rat islets, as demonstrated by an increase in Ki-67–positive cells to total β-cells in the MI-treated group (Fig. 7*H* and *I*).

To further elucidate the mechanism by which MI supplementation improves islet function, we characterized the intracellular PIP_2 levels in MI-treated and untreated ZDF rat islets. Results showed that ZDF control islets exhibited a remarkable reduction in PIP_2 level compared with that of lean rats, whereas MI supplementation partially restored the decreased intracellular PIP_2 level in ZDF rat islets (Fig. 7*J*). In addition, MI supplementation significantly elevated the basal phosphorylation level of AKT (Fig. 7*K*) and ERK (Fig. 7*L*). Moreover, MI-treated ZDF rat islets displayed an augmented insulin content (Fig. 7*M*) and percentage of insulin secreted from intracellular insulin content compared with the ZDF control rat islets (Fig. 7*N*).

DISCUSSION

In the current study, we report for the first time the expression of Na^+-dependent MI cotransporters in pancreatic islets and β-cells and provide a plausible molecular explanation for prior observations of active MI transport in pancreatic islets (12,13). The particularly strong expression of SMIT1 observed in this study suggests that there is a dominant role of SMIT1 in β-cell MI transport and that the effects of pharmacological SMIT inhibition with phlorizin can be attributed, at least in large part, to SMIT1. We obtained ex vivo and in vivo data showing that MI administration alone can improve islet function, potentiating insulin secretion in glucose-challenge experiments. Genetic knockdown of SMIT decreased expression of *Irs1* and increased expression of *Irs2*, consistent with a recent report showing that inhibition of insulin receptor substrate signaling elevates *Irs2* expression as a form of feedback regulation (32). On the basis of our findings, we have developed a novel molecular model of SMIT1-mediated regulation on PI signaling in pancreatic β-cells via manipulation on the intracellular PIP_2 level. Furthermore, we demonstrated that MI, being a cellular osmolyte and the precursor of PI, is involved in both osmoregulation and intracellular signaling events and regulates insulin secretion in pancreatic β-cells.

Osmoregulation in brain and kidney cells under hypertonic stress is known to require SMITs and MI (33,34), and previous studies have shown SMIT1 being upregulated in response to extracellular hypertonic stress in neural cells (35,36). Although β-cells are also prone to extracellular hypertonicity, their responses to fluid balance with regulatory mechanisms are not well characterized. Our view is that the presently observed upregulation of SMIT1 expression in response to acute hypertonic stress, resulting from transient high-glucose exposure or early-stage hyperglycemia, reflects an adaptive response; it is because MI transporter upregulation enables β-cells to accumulate osmolytes and thereby raises their intracellular osmolarity for the maintenance of cell volume and fluid balance. Such autoregulation of cell volume may be important for β-cell function given that hypotonicity alone has been shown to induce β-cell insulin release (37,38).

Because MI is a PI precursor, the MI transporter SMIT1 may influence intracellular signaling events by manipulating the PI pool. Our finding that knockdown of SMIT1 in INS-1E cells reduced intracellular PIP_2 levels in β-cells is consistent with prior study (i.e., increased SMIT1 activity raised intracellular levels of both MI and PI), thereby altering the behavior of PIP_2-dependent ion channels in ganglion neurons (33). Furthermore, we observed that knockdown of SMIT1 led to impaired downstream PIP_2 signaling, including $PIP_2/IP_3/Ca^{2+}$ and PI3K/Akt signaling, such that a reduction in AKT phosphorylation was observed and the transcription of genes that encode β-cell function regulating proteins was downregulated. Indeed, previous studies have reported that PI, being a major intracellular second messenger signaling molecule, has an important physiological role in β-cell function (39,40). In particular, PIP_2 generates two downstream effectors, diacylglycerol and IP_3; these effectors have been shown to regulate GSIS by promoting the maturation and exocytosis of insulin granules (41,42). PIP_3, a downstream counterpart of PIP_2, has also been shown to be involved in the regulation of GSIS as well as the proliferation and survival of β-cells through PI3K/Akt signaling (40). In light of these findings, our present data introduce a previously unidentified signaling cascade between SMIT1 and PI signaling in β-cells, which we have modeled in Fig. 8.

Interestingly, our data show that SMIT1 expression was downregulated in islets cultured under chronic high-glucose exposure and hyperglycemic conditions but augmented after acute high-glucose treatment. The data are indeed in comparison with different glycemic states of different stages during diabetic development. The ZDF rat is a well-established model for type 2 diabetes (43,44). Our data showed that although young ZDF rats attained normal fasting blood glucose levels at 6–8 weeks of age (stage 1), their random blood glucose levels were significantly elevated (Supplementary Fig. 5); by 9–12 weeks of age through ~20 weeks (stage 2), they become fully diabetic, with evident hyperglycemia and hyperinsulinemia (Supplementary Fig. 5); and from 20 weeks old onwards (stage 3), they become severely hyperglycemic, yet their plasma insulin concentrations reduced remarkably, as reported previously (43,44). It is surprising to identify that

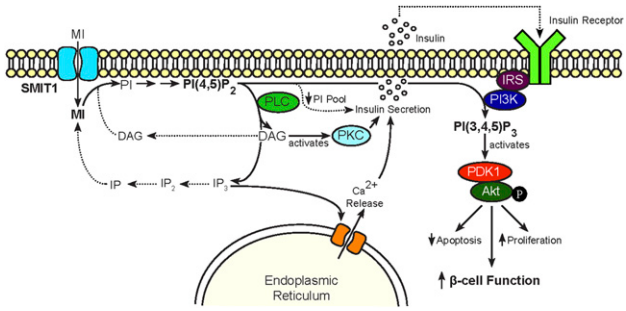

Figure 8—Schematic diagram summarizing a proposed molecular model for SMIT1 and PI signaling in pancreatic β-cells. SMIT1 transports MI into β-cells and in turn regulates the intracellular PIP_2 level and its subsequent downstream signaling cascades. PIP_2 potentiates insulin secretion by modulating the intracellular Ca^{2+} level, whereas PIP_3 regulates β-cell function and survival through activation of PI3K/Akt signaling pathway. DAG, diacylglycerol.

SMIT1 mRNA expression has already been upregulated when young ZDF rats display elevated random blood glucose levels. We postulate that this might be a compensatory mechanism by which the rat pancreatic islets adapt to the steeply rising demand for insulin secretion during the development of insulin resistance at that stage. Such upregulation was also observed in islets from the 11- to 12-week-old ZDF rats, inconsistent with the response toward hypertonic stress in high-glucose–treated INS-1E cells. On the contrary, SMIT1 mRNA expression was significantly downregulated in the islets from the 24- to 34-week-old ZDF rats. This reversal may represent a decompensated osmoregulation of β-cells under chronic high-glucose exposure, which may be relevant for elucidating the pathogenesis of type 2 diabetes.

Although our molecular model is suggestive of SMIT1-mediated regulation of PI signaling cascades, it is also possible that SMIT1 might modulate insulin secretion in β-cells through PIP_2-modulated effects on ion channel activities, similar to the SMIT1 regulation of ion channels in ganglion neurons (33). Our data showed that such regulatory events might also occur in β-cells given that PIP_2/PLC/IP_3 signaling, which regulates insulin secretion through intracellular Ca^{2+} modulation (14), was downregulated upon SMIT1 knockdown. Furthermore, reductions in PIP_2 have been shown to elevate basal β-cell insulin secretion by desensitizing K_{ATP} channels to intracellular ATP (45). However, to our surprise, basal insulin secretion was not augmented in our SMIT1 knocked-down INS-1E cells. Given prior data implicating the PI phosphorylation cycle in the regulation of PIP_2 turnover in β-cells (46), we postulate that a dramatic reduction in PIP_2 levels might be necessary to desensitize the K_{ATP} channels and that, in SMIT1 knocked-down cells, de novo synthesis of PIP_2 may compensate partially for such a PIP_2 loss. Molecular studies on the relationships between SMIT1, PIP_2, and K_{ATP} are necessary to test this hypothesis. Interestingly, the presently reported beneficial effects of MI supplementation on β-cell and islet function in diabetes are consistent with prior clinical studies showing that MI supplementation can prevent gestational diabetes (7–9), as well as with studies showing MI-related improvements in insulin sensitivity in diabetic mice (47,48). To this end, studies of SMIT1 knockout mice (49) could be used to further characterize the in vivo functional role of SMIT1 in rodent models.

In conclusion, given the relatively ubiquitous expression of SMIT1 (19,22), our data provide not only a new perspective on the pathophysiology of type 2 diabetes but also broad physiological significance with respect to molecular aspects of other diseases characterized by altered inositol metabolism.

Funding. This work was fully supported by the General Research Fund of The Research Grants Council of the Hong Kong Special Administrative Region, China (Ref. No.: CUHK14107415), awarded to P.S.L.

Duality of Interest. No potential conflicts of interest relevant to this article were reported.

Author Contributions. S.Y.T.L. designed and performed experiments, analyzed and interpreted data, and drafted the manuscript. S.T.W.C. and D.Z. performed experiments and analyzed data. P.S.L. designed the experiments, analyzed and interpreted data, and revised the manuscript. P.S.L. is the guarantor of this work and, as such, had full access to all of the data in the study and takes responsibility for the integrity of the data and the accuracy of the data analysis.

Prior Presentation. Parts of this study were presented in abstract form at the 75th Scientific Sessions of the American Diabetes Association, Boston, MA, 5–9 June 2015.

References

1. Michell RH. Inositol derivatives: evolution and functions. Nat Rev Mol Cell Biol 2008;9:151–161
2. Chau JF, Lee MK, Law JW, Chung SK, Chung SS. Sodium/myo-inositol cotransporter-1 is essential for the development and function of the peripheral nerves. FASEB J 2005;19:1887–1889
3. Dai Z, Chung SK, Miao D, Lau KS, Chan AW, Kung AW. Sodium/myo-inositol cotransporter 1 and myo-inositol are essential for osteogenesis and bone formation. J Bone Miner Res 2011;26:582–590
4. Ostlund RE Jr, McGill JB, Herskowitz I, Kipnis DM, Santiago JV, Sherman WR. D-chiro-inositol metabolism in diabetes mellitus. Proc Natl Acad Sci U S A 1993;90:9988–9992
5. Baillargeon JP, Diamanti-Kandarakis E, Ostlund RE Jr, Apridonidze T, Iuorno MJ, Nestler JE. Altered D-chiro-inositol urinary clearance in women with polycystic ovary syndrome. Diabetes Care 2006;29:300–305
6. Hong JH, Jang HW, Kang YE, et al. Urinary chiro- and myo-inositol levels as a biological marker for type 2 diabetes mellitus. Dis Markers 2012;33:193–199
7. Celentano C, Matarrelli B, Mattei PA, Pavone G, Vitacolonna E, Liberati M. Myo-inositol supplementation to prevent gestational diabetes mellitus. Curr Diab Rep 2016;16:30
8. Santamaria A, Di Benedetto A, Petrella E, et al. Myo-inositol may prevent gestational diabetes onset in overweight women: a randomized, controlled trial. J Matern Fetal Neonatal Med 2015;29:3234–3237
9. D'Anna R, Scilipoti A, Giordano D, et al. myo-Inositol supplementation and onset of gestational diabetes mellitus in pregnant women with a family history of type 2 diabetes: a prospective, randomized, placebo-controlled study. Diabetes Care 2013;36:854–857
10. Handler JS, Kwon HM. Regulation of the myo-inositol and betaine co-transporters by tonicity. Kidney Int 1996;49:1682–1683
11. Prpić V, Blackmore PF, Exton JH. myo-Inositol uptake and metabolism in isolated rat liver cells. J Biol Chem 1982;257:11315–11322

12. Biden TJ, Wollheim CB. Active transport of myo-inositol in rat pancreatic islets. Biochem J 1986;236:889–893
13. Pace CS, Clements RS. Myo-inositol and the maintenance of beta-cell function in cultured rat pancreatic islets. Diabetes 1981;30:621–625
14. Zawalich WS, Zawalich KC, Kelley GG. Regulation of insulin release by phospholipase C activation in mouse islets: differential effects of glucose and neurohumoral stimulation. Endocrinology 1995;136:4903–4909
15. Assmann A, Ueki K, Winnay JN, Kadowaki T, Kulkarni RN. Glucose effects on beta-cell growth and survival require activation of insulin receptors and insulin receptor substrate 2. Mol Cell Biol 2009;29:3219–3228
16. Hakonen E, Ustinov J, Eizirik DL, Sariola H, Miettinen PJ, Otonkoski T. In vivo activation of the PI3K-Akt pathway in mouse beta cells by the EGFR mutation L858R protects against diabetes. Diabetologia 2014;57:970–979
17. Balla T. Phosphoinositides: tiny lipids with giant impact on cell regulation. Physiol Rev 2013;93:1019–1137
18. Kwon HM, Yamauchi A, Uchida S, et al. Cloning of the cDNa for a Na+/myo-inositol cotransporter, a hypertonicity stress protein. J Biol Chem 1992;267:6297–6301
19. Berry GT, Mallee JJ, Kwon HM, et al. The human osmoregulatory Na+/myo-inositol cotransporter gene (SLC5A3): molecular cloning and localization to chromosome 21. Genomics 1995;25:507–513
20. Coady MJ, Wallendorff B, Gagnon DG, Lapointe JY. Identification of a novel Na+/myo-inositol cotransporter. J Biol Chem 2002;277:35219–35224
21. Bissonnette P, Lahjouji K, Coady MJ, Lapointe JY. Effects of hyper-osmolarity on the Na+ -myo-inositol cotransporter SMIT2 stably transfected in the Madin-Darby canine kidney cell line. Am J Physiol Cell Physiol 2008;295: C791–C799
22. Chen J, Williams S, Ho S, et al. Quantitative PCR tissue expression profiling of the human SGLT2 gene and related family members. Diabetes Ther 2010;1:57–92
23. Cheng Q, Law PK, de Gasparo M, Leung PS. Combination of the dipeptidyl peptidase IV inhibitor LAF237 [(S)-1-[(3-hydroxy-1-adamantyl)ammo]acetyl-2-cyanopyrrolidine] with the angiotensin II type 1 receptor antagonist valsartan [N-(1-oxopentyl)-N-[[2′-(1H-tetrazol-5-yl)-[1,1′-biphenyl]-4-yl]methyl]-L-valine] enhances pancreatic islet morphology and function in a mouse model of type 2 diabetes. J Pharmacol Exp Ther 2008;327:683–691
24. Smelt MJ, Faas MM, de Haan BJ, de Vos P. Pancreatic beta-cell purification by altering FAD and NAD(P)H metabolism. Exp Diabetes Res 2008;2008:165360
25. Clardy SM, Mohan JF, Vinegoni C, et al. Rapid, high efficiency isolation of pancreatic β-cells. Sci Rep 2015;5:13681
26. Merglen A, Theander S, Rubi B, Chaffard G, Wollheim CB, Maechler P. Glucose sensitivity and metabolism-secretion coupling studied during two-year continuous culture in INS-1E insulinoma cells. Endocrinology 2004;145:667–678
27. Leung KY, Mills K, Burren KA, Copp AJ, Greene ND. Quantitative analysis of myo-inositol in urine, blood and nutritional supplements by high-performance liquid chromatography tandem mass spectrometry. J Chromatogr B Analyt Technol Biomed Life Sci 2011;879:2759–2763
28. Gray A, Olsson H, Batty IH, Priganica L, Peter Downes C. Nonradioactive methods for the assay of phosphoinositide 3-kinases and phosphoinositide phosphatases and selective detection of signaling lipids in cell and tissue extracts. Anal Biochem 2003;313:234–245
29. Hager K, Hazama A, Kwon HM, Loo DD, Handler JS, Wright EM. Kinetics and specificity of the renal Na+/myo-inositol cotransporter expressed in Xenopus oocytes. J Membr Biol 1995;143:103–113
30. Kitamura T, Nakae J, Kitamura Y, et al. The forkhead transcription factor Foxo1 links insulin signaling to Pdx1 regulation of pancreatic beta cell growth. J Clin Invest 2002;110:1839–1847
31. Meur G, Qian Q, da Silva Xavier G, et al. Nucleo-cytosolic shuttling of FoxO1 directly regulates mouse Ins2 but not Ins1 gene expression in pancreatic beta cells (MIN6). J Biol Chem 2011;286:13647–13656
32. Tsunekawa S, Demozay D, Briaud I, et al. FoxO feedback control of basal IRS-2 expression in pancreatic β-cells is distinct from that in hepatocytes. Diabetes 2011;60:2883–2891
33. Dai G, Yu H, Kruse M, Traynor-Kaplan A, Hille B. Osmoregulatory inositol transporter SMIT1 modulates electrical activity by adjusting PI(4,5)P2 levels. Proc Natl Acad Sci U S A 2016;113:E3290–E3299
34. Yamauchi A, Nakanishi T, Takamitsu Y, et al. In vivo osmoregulation of Na/myo-inositol cotransporter mRNA in rat kidney medulla. J Am Soc Nephrol 1994;5:62–67
35. Lien YH, Shapiro JI, Chan L. Effects of hypernatremia on organic brain osmoles. J Clin Invest 1990;85:1427–1435
36. Yamashita T, Tamatani M, Taniguchi M, Takagi T, Yoshimine T, Tohyama M. Regulation of Na+/myo-inositol cotransporter gene expression in hyperglycemic rat hippocampus. Brain Res Mol Brain Res 1998;57:167–172
37. Straub SG, Daniel S, Sharp GW. Hyposmotic shock stimulates insulin secretion by two distinct mechanisms. Studies with the betaHC9 cell. Am J Physiol Endocrinol Metab 2002;282:E1070–E1076
38. Bacová Z, Orecná M, Hafko R, Strbák V. Cell swelling-induced signaling for insulin secretion bypasses steps involving G proteins and PLA2 and is N-ethylmaleimide insensitive. Cell Physiol Biochem 2007;20:387–396
39. Yamazaki H, Zawalich KC, Zawalich WS. Physiologic implications of phosphoinositides and phospholipase C in the regulation of insulin secretion. J Nutr Sci Vitaminol (Tokyo) 2010;56:1–8
40. Rameh LE, Deeney JT. Phosphoinositide signalling in type 2 diabetes: a β-cell perspective. Biochem Soc Trans 2016;44:293–298
41. Kabachinski G, Yamaga M, Kielar-Grevstad DM, Bruinsma S, Martin TF. CAPS and Munc13 utilize distinct PIP2-linked mechanisms to promote vesicle exocytosis. Mol Biol Cell 2014;25:508–521
42. Berridge MJ, Irvine RF. Inositol phosphates and cell signalling. Nature 1989; 341:197–205
43. Shiota M, Printz RL. Diabetes in Zucker diabetic fatty rat. Methods Mol Biol 2012;933:103–123
44. Lee Y, Hirose H, Ohneda M, Johnson JH, McGarry JD, Unger RH. Beta-cell lipotoxicity in the pathogenesis of non-insulin-dependent diabetes mellitus of obese rats: impairment in adipocyte-beta-cell relationships. Proc Natl Acad Sci U S A 1994;91:10878–10882
45. Lin CW, Yan F, Shimamura S, Barg S, Shyng SL. Membrane phosphoinositides control insulin secretion through their effects on ATP-sensitive K+ channel activity. Diabetes 2005;54:2852–2858
46. Thore S, Wuttke A, Tengholm A. Rapid turnover of phosphatidylinositol-4,5-bisphosphate in insulin-secreting cells mediated by Ca2+ and the ATP-to-ADP ratio. Diabetes 2007;56:818–826
47. Croze ML, Vella RE, Pillon NJ, et al. Chronic treatment with myo-inositol reduces white adipose tissue accretion and improves insulin sensitivity in female mice. J Nutr Biochem 2013;24:457–466
48. Croze ML, Géloën A, Soulage CO. Abnormalities in myo-inositol metabolism associated with type 2 diabetes in mice fed a high-fat diet: benefits of a dietary myo-inositol supplementation. Br J Nutr 2015;113:1862–1875
49. Bersudsky Y, Shaldubina A, Agam G, Berry GT, Belmaker RH. Homozygote inositol transporter knockout mice show a lithium-like phenotype. Bipolar Disord 2008;10:453–459